Journal of Thermal Analysis and Calorimetry, Vol. 77 (2004) 653–662

THERMAL AND STRUCTURAL PROPERTIES OF AMBROXOL POLYMORPHS

M. R. Caira[1], *A. Foppoli*[2], *M. E. Sangalli*[2], *L. Zema*[2] *and F. Giordano*[3*]

[1]Department of Chemistry, University of Cape Town, Rondebosch 7701, Cape Town, South Africa
[2]Istituto di Chimica Farmaceutica e Tossicologica, Università di Milano, Viale Abruzzi 42, 20131 Milano, Italy
[3]Dipartimento Farmaceutico, Università di Parma, Parco Area delle Scienze, 43100 Parma, Italy

Abstract

The thermal and structural characteristics of two crystal forms of ambroxol, (*trans*-((amino-2-dibromo-3,5-benzyl)amino)-4-cyclohexanol), a drug with remarkable mucolytic and expectorant properties marketed in several drug products, were investigated.

Form II (*m.p*. 92.4°C) is obtained by spontaneous cooling from a hot water/ethanol solution while Form I (*m.p*. 99.5°C) slowly separates from the mother liquor. The two forms can be identified by PXRD and DSC analyses. On the basis of both thermal and structural data the thermodynamic relationship of enantiotropy was deduced. No metastable (Form I)→stable (Form II) conversion was observed upon storage at ambient conditions. Form I crystallizes in the space group $P2_1/n$ (alternative setting of $P2_1/c$) with Z=8. Form II crystallizes in the space group $P2_1/c$ with Z=4 and a significantly different crystal packing arrangement from that in Form I. A third crystalline modification, Form III (space group $P2_1/c$ with Z=16) was detected on cooling a single crystal of Form I down to –70°C. On warming to ambient temperature Form III was found to revert to Form I. This reversible single crystal to single crystal transition was structurally characterised and found to involve subtle changes in the types and extent of molecular disorder as well as the hydrogen bonding arrangement.

Keywords: ambroxol, crystal structure, polymorphism, thermal analysis

Introduction

Polymorphism is achieving a growing interest from the pharmaceutical companies since solid-state properties can differ dramatically from one polymorph to another and, as a consequence, manufacturability, bioavailability and stability of a drug product can be severely conditioned when new or unexpected crystal phases of the active ingredient or even of the excipients are involved. This leads to the need for a thorough preliminary characterization of the solid-state properties of each component within the pharmaceutical formulation, aiming to deal always with the same polymorph, for drugs and excipients, when manufacturing drug products [1].

* Author for correspondence: E-mail: giordano@unipr.it

1388–6150/2004/ $ 20.00

Akadémiai Kiadó, Budapest
Kluwer Academic Publishers, Dordrecht

Ambroxol, (*trans*-((amino-2-dibromo-3,5-benzyl)amino)-4-cyclohexanol, AMB) (Fig. 1), is used in medical practice as mucolytic and expectorant drug and recently has been also proposed for the treatment of pulmonary alveolar proteinosis [2] and of the sicca keratoconjunctivitis associated with Sjögren syndrome [3].

The present paper describes for the first time the solid-state properties of two polymorphs (I, II) of ambroxol. The crystal forms were investigated by thermal analysis (DSC, TG, HSM) and X-ray diffractometry on powder and on single crystals. An outline of the thermodynamic relationship between ambroxol solid phases is also given. The detection of a third polymorph (III) at low temperature and its structural relationship with (I) are also described.

Experimental

Materials and methods

AMB hydrochloride was purchased from ICN Biomedicals and used as received. All solvents used were of analytical purity grade.

AMB (free base) was obtained by dissolving AMB hydrochloride in water (13 g L^{-1} at 60°C) and by adding dropwise, under stirring, aqueous NaOH (4% by mass) up to a pH value of ~9.5. The resulting suspension was then allowed to stand overnight at 4°C and suction filtered. The recovered solid was thoroughly washed with cold water and air dried at ambient temperature.

Physicochemical data of AMB (elemental analysis, FTIR and NMR spectra) were consistent with the structural formula shown in Fig. 1. The yield was practically quantitative.

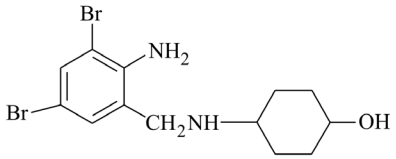

Fig. 1 Structural formula of AMB

Recrystallizations were conducted by dissolving approximately 250 mg samples in the minimum amount of the solvent (water, ethanol and their 1:1 *v/v* mixture) at temperatures a few degrees below the boiling point of the solvent. The saturated solution was then filtered while hot (0.45 μm nylon microfilter) and left to recrystallize by spontaneous cooling at room temperature. Recrystallized products were isolated by suction filtration and air-dried at ambient temperature prior to solid-state analyses.

Differential scanning calorimetry (DSC) and thermogravimetric analysis (TG): scans were acquired with TA Instruments equipments (DSC2010 calorimeter, TG2050 thermobalance) under nitrogen purging of 70 mL min^{-1}. DSC runs were performed on 2–3 mg samples in non-hermetically sealed aluminum pans at scanning rates within the 1–10 K min^{-1} range; TG was performed on 15–20 mg samples at 5 K min^{-1}.

Hot stage microscopy (HSM): a hot stage apparatus HSF 91 Linkam Scientific Instruments equipped with a microscope (Labophot II polarising microscope, Nikon) was used as supplementary source of information. A 3CCD color video camera module (XC-003P Sony), supported by Image-Pro® Plus 4.0 software, allowed the recording of images during temperature scans.

X-ray diffractometry on powder (PXRD) and on single crystal: PXRD patterns were recorded on a Philips PW1080/50 vertical goniometer with CuK_α-radiation (λ=1.5418 Å) on finely ground samples. Step-scans of 0.1° 2θ and 4 s counts per step were employed. Single crystals were mounted on a Nonius Kappa CCD diffractometer and intensity data were collected at ambient temperature for Forms I and II using a combination of ϕ- and ω-scans. Cooling of Form I to –70°C in a stream of nitrogen vapour effected a crystal transformation and intensity data were collected for the new phase (Form III). All data were corrected for Lorentz-polarization effects as well as absorption. The crystal structures were solved by direct methods [4] and refined by full-matrix least-squares [5] *vs*. F^2. Molecular disorder detected in Forms I and III was treated by assigning appropriate site-occupancy factors to the components of disordered residues. Ordered non-H atoms were treated anisotropically. All H atoms were located and were generally placed in idealized positions in a riding model with U_{iso}=1.2 times those of their parent atoms. H atoms of the amine and hydroxyl groups were allowed to refine freely subject only to appropriate distance constraints. In the final refinements least-squares weights of the form $w=[\sigma^2(F_o^2)+(aP)^2+bP]^{-1}$ where $P=[\max(F_0^2, 0)+2F_c^2]/3$ were employed.

Complete crystallographic data for the three polymorphs have been deposited at the Cambridge Crystallographic Data Centre (Deposition Numbers: CCDC 234307 - 234309).

Results and discussion

Single polymorphs of AMB can be isolated from water–ethanol 1:1 mixtures, depending on the recrystallization procedure. When the hot solution is allowed to cool spontaneously to ambient temperature, a microcrystalline precipitate (AMB I) is obtained. On standing for several days, long thin needles of AMB II separate from the filtrate. From pure solvents, both water and ethanol, Form I was always isolated.

X-ray powder diffractometry

PXRD patterns of the two polymorphs are drawn in Fig. 2. Both traces are characterized by numerous and sharp peaks revealing the highly crystalline nature of the samples. Distinct differences in the profiles of the two modifications are evident and in particular characteristic diffraction peaks can be observed at 7.1 and 20.6° (2θ) for Form I and at 7.4, 8.3, 14.8, 22.7 and 30.0° (2θ) for Form II.

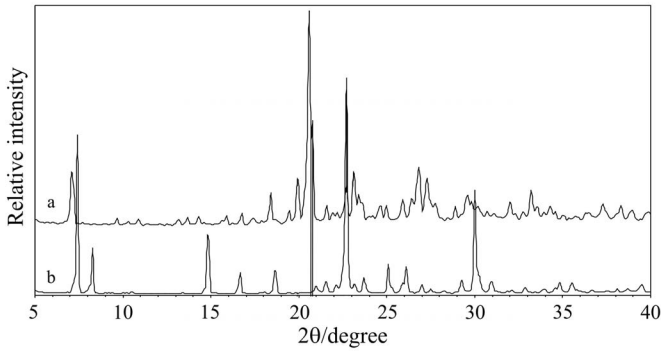

Fig. 2 PXRD patterns of a – AMB I and b – AMB II polymorphs

Thermal analysis

The DSC traces of both polymorphs and their mixture (occasionally obtained by rapid cooling of the hot water/ethanol solution) are depicted in Fig. 3. In the temperature interval under investigation, pure polymorphs show a single endothermic melting peak at about 100 and 94°C (T_{peak}) for Form I and Form II, respectively; no baseline displacement was observed below and above the melting peaks thus suggesting a remarkable thermal stability of AMB in the liquid phase. No mass loss was observed by TG within the same temperature range, thus excluding the presence of pseudopolymorphs.

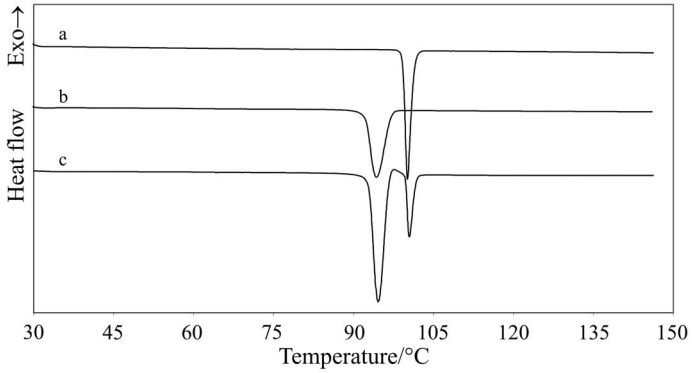

Fig. 3 DSC curves of a – AMB I and b – AMB II polymorphs and c – their 1:4 mixture; scanning rate: 5 K min^{-1}

The average melting point and heat of fusion values for both forms are provided in Table 1. According to the heat of fusion rule by Burger and Ramberger, since the higher melting polymorph shows the lower heat of fusion, the two forms are enantiotropically related [6]. The transition temperature, inferred from melting data, according to Yu [7], is 58°C; therefore Form II is the thermodynamically stable polymorph at ambient temperature and Form I the metastable one. This conclusion is

Table 1 Thermal data of AMB polymorphs

	Melting point*/°C; (s.d.), *n*=3	Heat of fusion/J g^{-1}; (s.d.), *n*=3
AMB I	99.5 (0.3)	83.2 (2.3)
AMB II	92.4 (0.1)	96.6 (2.0)

*extrapolated onset temperature; scanning rate, 5 K min^{-1}

also supported by the solvent-mediated conversion of Form I into Form II upon suspension of the former in water at room temperature.

When testing mixtures of both polymorphs, the DSC scan recorded at 5 K min^{-1} (Fig. 3c), besides the melting endotherms of each form, displays an exothermic peak just above the melting temperature of Form II; this peak, as confirmed by HSM observations, is associated with the rearrangement/crystal growth of Form I from the molten phase. The extent of this phenomenon is affected by the heating rate selected for the DSC scan; specifically, on lowering the heating rate down to 2.5, or 1 K min^{-1} (Fig. 4), both the exothermic peak of recrystallization and the endothermic peak relevant to melting of Form I tend to increase.

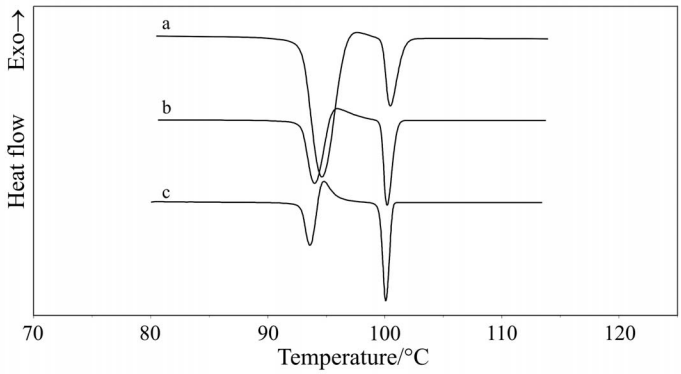

Fig. 4 DSC curves of AMB polymorphs mixture recorded at different scanning rates: a – 5, b – 2.5 and c – 1 K min^{-1}

Furthermore, since the DSC patterns recorded on Form II samples at the same heating rates (range, 1–5 K min^{-1}) do not show any exothermic peak, the recrystallization of Form I from the liquid most likely depends on the presence of Form I seeds. Therefore, DSC analysis performed at appropriate heating rates can represent a suitable method for the evaluation of AMB Form I–Form II mixtures.

Molten AMB fails to recrystallize on cooling and a glassy amorphous phase is obtained, which, on heating (scanning rate, 5 K min^{-1}), shows a pseudoendothermic event at ~18°C corresponding to the glassy-rubbery transition (Fig. 5). At approximately 85°C the exothermic crystallization of the rubbery amorphous phase

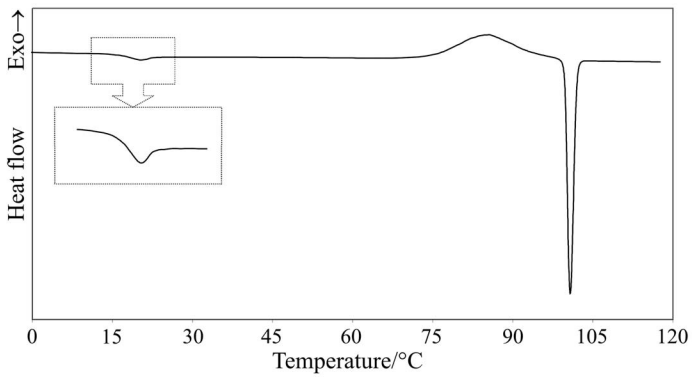

Fig. 5 DSC curve of amorphous AMB; scanning rate 5 K min^{-1}

as Form I occurs, as demonstrated by the final melting event. In no case could AMB Form II be isolated from the melt, thus confirming that Form I is the thermodynamically stable solid phase at high temperature, since it can be isolated above the Form II→Form I transition temperature.

X-ray diffractometry on single crystal

Crystals of AMB I were grown from the saturated water/ethanol solution by slow evaporation. Crystals of AMB II suitable for structural analysis could be recovered from a saturated solution in absolute ethanol by spontaneous cooling.

Crystal data for the polymorphs are listed in Table 2. The crystallographic asymmetric unit in Form I comprises two molecules of ambroxol A, B (Fig. 6, I). While molecule A is ordered, two alternative sites for the methylene (C10) and

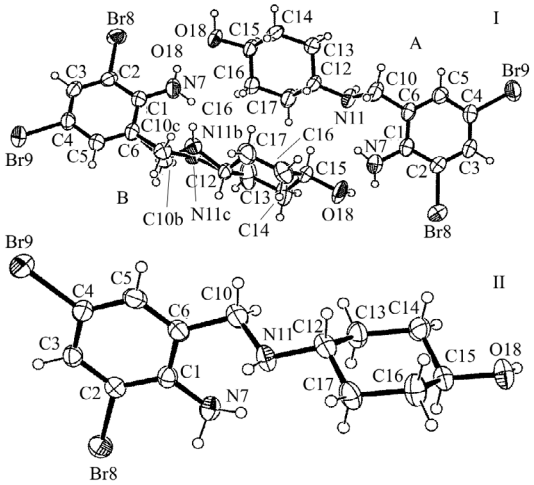

Fig. 6 The crystallographic asymmetric units in Forms I and II. Thermal ellipsoids are drawn at the 40% probability level

bonded secondary amine (N11) groups, with equal statistical occupancies, were evident in molecule B. In addition, the phenyl and cyclohexyl rings have different dispositions in the two independent molecules. To test whether the disorder was specimen-dependent, complete X-ray analysis of a second crystal of Form I taken from a different preparation was carried out. Identical structural features were observed, implying that they are inherent to this polymorph. Molecules in Form I assemble in layers (Fig. 7) within which there is extensive hydrogen bonding, shown separately for a representative layer. A dimer is formed between molecules A and B via head-to-tail hydrogen bonding (O18B-H···N7A, N7B-H···O18A). These dimers are in turn linked along the crystal *b*-axis by a hydrogen bond O18A-H···O18B. Also shown in Fig. 7 is an intramolecular hydrogen bond N7-H···N11 which occurs in both molecules of the asymmetric unit. The layered structure of Form I is responsible for the intense peak at $2\theta=20.7°$ in the PXRD pattern (Fig. 2a). Indexing of the pattern confirmed that the strongest contributor to this peak is the 004 reflection and Fig. 7 shows that the molecular layers lie midway between these planes. These layers are held together by van der Waals forces only.

Table 2 Crystal data and refinement parameters for AMB polymorphs

Parameter	Form I	Form II	Form III
Crystal system	monoclinic	monoclinic	monoclinic
Space group	$P2_1/n$	$P2_1/c$	$P2_1/c$
a/Å	16.2064(2)	12.100(2)	22.5601(2)
b/Å	10.6651(1)	23.636(5)	10.5120(1)
c/Å	17.2444(2)	5.156(1)	24.7743(3)
β/°	94.84(1)	100.36(3)	92.40(1)
V/Å^3	2969.94(6)	1450.4(5)	5870.1(1)
Z	8	4	16
D_c/g cm^{-3}	1.691	1.732	1.711
Crystal size/mm^3	0.18×0.18×0.07	0.10×0.07×0.05	0.12×0.10×0.07
Crystal shape	block	block	block
μ/mm^{-1}	5.45	5.52	5.58
T/K	294(2)	294(2)	203(2)
Reflections msd.	52456	30850	124314
Data/restraints/ parameters	6748/4/344	3194/3/179	12447/28/697
R_1 [$I>2\sigma(I)$]	0.0451	0.0493	0.0517
wR2 [$I>2\sigma(I)$]	0.0901	0.1132	0.1022
S (goodness-of-fit)	1.020	1.053	1.066
Max. shift/e.s.d.	0.001	<0.001	0.002
$\Delta\rho_{max}$/e Å^{-3}	0.66	1.15	1.38

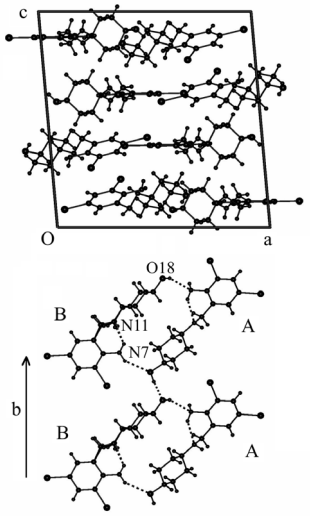

Fig. 7 Crystal structure of Form I showing molecular layers (top) and hydrogen bonds within a layer (bottom)

In the crystal of Form II, the asymmetric unit is a single, ordered molecule of AMB (Fig. 6, II), with a conformation similar to that of molecule B in Form I. The crystal structure of Form II (Fig. 8) features isolated domains of *c*-glide related molecules hydrogen bonded head-to-head via O18-H···O18^{i} hydrogen bonds (*i*=*x*, 1.5-*y*, 0.5+*z*) as well as N11-H···N7^{ii} hydrogen bonds (*ii*=*x, y*, –1+*z*) that link molecules related by translation along the *c*-axis. The same intramolecular hydrogen bond (N11-H···N7) occurring in Form I is found in Form II. In the computed PXRD pattern of Form II (not shown) there is a reversal in the intensities of the two strongest peaks of Fig. 2b. This indicates some degree of preferred orientation in the sample,

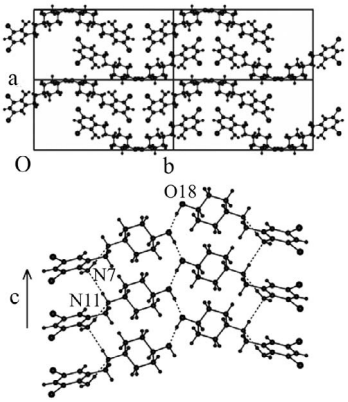

Fig. 8 Crystal structure of Form II and hydrogen bonding between *c*-glide related molecules and those translated along *c*

consistent with the pronounced acicular habit of this Form. The most intense peak in the computed pattern, at 2θ=7.4°, is due to the 020 reflection and Fig. 8 shows that the 020 crystal planes are straddled by strongly diffracting bromine atoms.

Relating the crystal structures of Forms I and II to the results of thermal analyses enables us to conclude that at ambient temperature the more symmetrical arrangement, Form II, with 4 ordered molecules in the unit cell, is the thermodynamically stable phase, while in the temperature domain above the calculated transition temperature (58°C), the stable phase is a less symmetrical crystal (Form I) with 4 ordered and 4 disordered molecules in the unit cell. The phase stable at higher temperature is also that containing molecules spanning a wider conformational range.

Slow cooling of a single crystal of Form I on the diffractometer from 24°C (at which temperature this phase is metastable with respect to Form II) to –70°C over a period of 2 h led to a single crystal to single crystal transformation to Form III. The unit cell of this phase is double that of Form I and therefore contains 16 molecules (Table 2). Since the space group is retained, the asymmetric unit now comprises 4 independent molecules (Fig. 9), three of which (A, B, C) are ordered, while the fourth (D) displays two alternative orientations of the cyclohexyl ring. Comparison of the hydrogen bonding in Forms I and III reveals another interesting change accompanying the transition. The 'A–B' dimer of Form I is replaced by two independent dimers 'A–B' and 'C–D' in Form III. In the latter phase, the hydrogen bonding in dimer 'A–B' is retained (Fig. 7) but

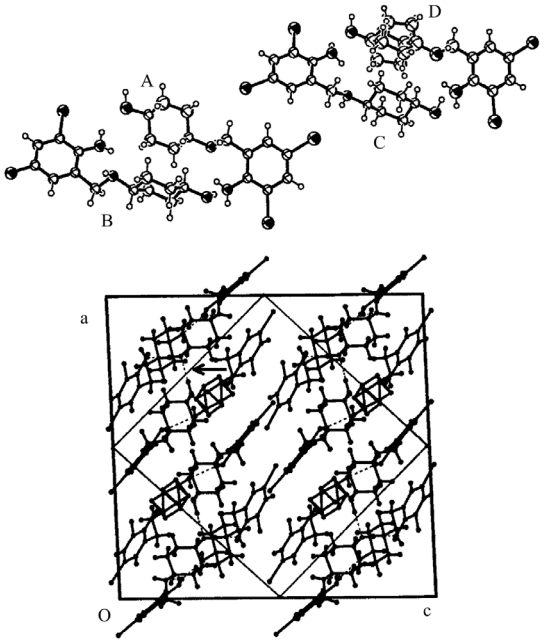

Fig. 9 The four independent molecules in the asymmetric unit of Form III and layered structure. The unit cell drawn with thin lines represents that of Form I, for reference. Inter-layer H-bonding is indicated by the arrow

in 'C–D', however, the hydroxyl group of molecule C no longer shows hydrogen bonds within the layer, but is rotated (Fig. 9) so as to form a hydrogen bond with an oxygen atom in the adjacent layer. These inter-layer hydrogen bonds exist between every successive pair of layers (Fig. 9). The subtle structural changes accompanying the transformation Form I→Form III thus include a reduction in the level of molecular disorder (from 1:2 in Form I to 1:4 in Form III) as well as a switch from exclusively intra-layer hydrogen bonding to a mixture of intra- and inter-layer hydrogen bonding. This remarkable transformation is reversible, as confirmed by the reappearance of Form I on slow warming of Form III to ambient temperature. Since Form III is only relevant at low temperature, it has little pharmaceutical relevance. It is nevertheless of considerable interest in the context of order-disorder transitions and crystal isostructurality [8], and its detection and relationship to Form I contribute to a more comprehensive picture of the polymorphism of AMB. Finally, as expected from the above description of Form III, its computed PXRD pattern closely resembles that of Form I, with the strongest reflection at $2\theta=20.9°$. This again corresponds to the separation of the molecular layers which in Form III are identified with the $4\ 0\ \bar{4}$ planes.

* * *

MRC acknowledges research support from the University of Cape Town and The National Research Foundation (Pretoria). MES, AF, LZ and FG gratefully acknowledge financial support of Italian MIUR and CNR.

References

1 D. Giron, J. Therm. Anal. Cal., 68 (2002) 335.
2 H. Suyama, N. Burioka, T. Sako, Y. Kawasaki, Y. Hitsuda, K. Shigeshiro and Y. Matsumoto, Yonago Acta Medica, 42 (1999) 175.
3 F. Segura-Lozano and G. Tenorio, Rev. Med. Hosp. Gen. Mex., 58 (1995) 118.
4 G. M. Sheldrick, SHELXS86, (G. M. Kruger, R. Goddard, Eds) In: Crystallographic computing 3. Oxford University Press, Oxford, UK 1985, p. 175.
5 G. M. Sheldrick, SHEXL97: Program for the refinement of crystal structures, University of Göttingen, Göttingen 1997.
6 A. Burger and R. Ramberger, Microchim. Acta, (1979) 259.
7 L. Yu, J. Pharm. Sci., 84 (1995) 966.
8 M. R. Caira, G. Bettinetti, M. Sorrenti and L. Catenacci, J. Pharm. Sci., 92 (2003) 2164.